Published online January 9, 2004

278–286 Nucleic Acids Research, 2004, Vol. 32, No. 1
DOI: 10.1093/nar/gkh171

Detection of guanine–adenine mismatches by surface plasmon resonance sensor carrying naphthyridine–azaquinolone hybrid on the surface

Shinya Hagihara[1], Hiroyuki Kumasawa[1], Yuki Goto[1], Gosuke Hayashi[1], Akio Kobori[2], Isao Saito[1] and Kazuhiko Nakatani[1,2,*]

[1]Department of Synthetic Chemistry and Biological Chemistry, Faculty of Engineering, Kyoto University, Kyoto, Japan and [2]PRESTO, Japan Science and Technology Agency (JST), Kyoto 615-8510, Japan

Received July 18, 2003; Revised October 15, 2003; Accepted November 15, 2003

ABSTRACT

We have discovered a new molecule naphthyridine–azaquinolone hybrid (Npt–Azq) that strongly stabilized the guanine-adenine (G-A) mismatch in duplex DNA. In the presence of Npt–Azq, the melting temperature (T_m) of 5′-d(CTA ACG GAA TG)-3′/3′-d(GAT TGA CTT AC)-5′ containing a single G-A mismatch increased by 15.4°C, whereas fully matched duplex increased its T_m only by 2.2°C. Npt–Azq was immobilized on the sensor surface for the surface plasmon resonance (SPR) assay to examine SPR detection of duplexes containing a G-A mismatch. Distinct SPR signals were observed when 27mer DNA containing a G-A mismatch was analyzed by the Npt–Azq immobilized sensor surfaces, whereas the signal of the fully matched duplex was ~6-fold weaker in intensity. The SPR signals for the G-A mismatch were proportional to the concentration of DNA in a range up to 1 μM, confirming that the SPR signal is in fact due to the binding of the G-A mismatch to Npt–Azq immobilized on the surface. Examination of all 16 G-A mismatches regarding the flanking sequence revealed that the sensor surface reported here is applicable to eight flanking sequences, covering 50% of all possible G-A mismatches.

INTRODUCTION

As a follow-on to the complete sequencing of the human genome, typing of single nucleotide polymorphisms (SNPs) in an array of disease-related genes is expected to be an indispensable technique for realizing personalized medicine. A number of methods have been developed for SNP typing (1–3), but much study is still needed to design new typing methods that are simple in operation, rapid and accurate in analysis, and low in cost. One of the challenges we have focused on is the reduction and eventual redundancy of labeled oligonucleotides for analysis. The expense of fluorescently labeling oligonucleotides and PCR products limits their application in large-scale typing by many currently available methods. We have reported a conceptually novel method of SNP typing that detects mismatch-containing duplexes with a small molecular ligand immobilized on a gold surface (4). Hybridization of two sets of duplex DNAs that differ from each other by a single nucleotide produces a DNA heteroduplex containing a single mismatched site. Mismatch-containing duplexes can be separated from homoduplexes by either gel electrophoresis (5,6), chemical and enzymatic cleavages at the mismatched site (7–9), or selective capture with mismatch-binding proteins (10,11). While these heteroduplex analyses applied to low-throughput screening are essentially free from oligonucleotide labeling, new technologies for high-throughput analyses are yet to be established. A small molecular ligand that selectively binds to a mismatched site could replace mismatch-binding proteins and bring an innovation to heteroduplex analyses (5,12–20). The ligand naphthyridine dimer (**Npt–Npt**) strongly and selectively binds to guanine–guanine mismatches in duplex DNA (5,12) (Fig. 1). The binding constant to a G-G mismatch in the 5′-CGG-3′/3′-GGC-5′ sequence is 1.9×10^7 M^{-1}. **Npt–Npt** consisting of two 2-amino-1,8-naphthyridine (**Npt**) chromophores, and a linker connecting the chromophores is designed so that each **Npt** produces three hydrogen bonds to each one of the guanines in the G-G mismatch, and the resultant naphthyridine–guanine pair is stabilized by stacking with the flanking base pairs. The proposed binding of **Npt–Npt** to the G-G mismatch has been verified by the 2D-NOESY spectrum of the complex (12). In addition to **Npt–Npt**, ligands that selectively and strongly bind to G-A, G-T and A-A mismatches are needed to accomplish SNP typing by a mismatch binding ligand. Taking into account the structure of **Npt–Npt** as a clue for the molecular design of ligands binding to a G-A mismatch, we have discovered naphthyridine–azaquinolone hybrids (**Npt–Azq**) where one **Npt** chromophore in **Npt–Npt** is replaced by a 8-azaquinolone chromophore (**Azq**) having complementary hydrogen-bonding surfaces to adenine (Fig. 2). Herein, we report the remarkable stabilization of G-A mismatch DNA by **Npt–Azq** and the first synthesis of a surface plasmon resonance (SPR) sensor detecting a G-A mismatch by immobilization of **Npt–Azq** on a gold surface.

*To whom correspondence should be addressed. Tel: +81 75 383 2756; Fax: +81 75 383 2759; Email: nakatani@sbchem.kyoto-u.ac.jp

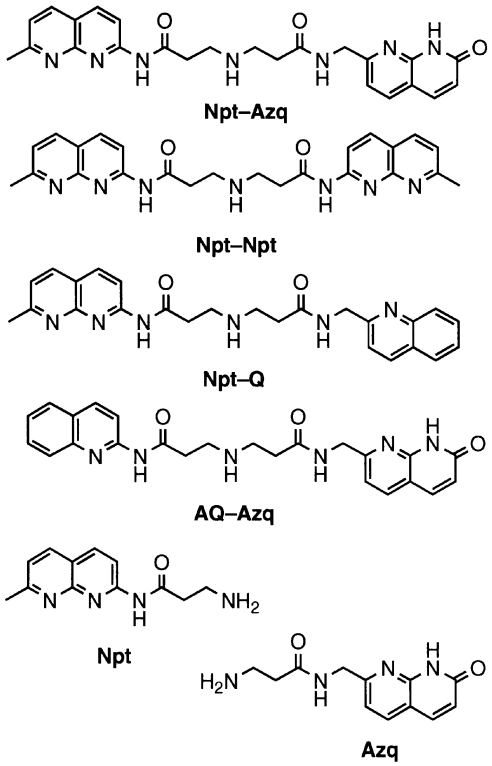

Figure 1. Formulas of **Npt**- and **Azq**-based hybrid molecules.

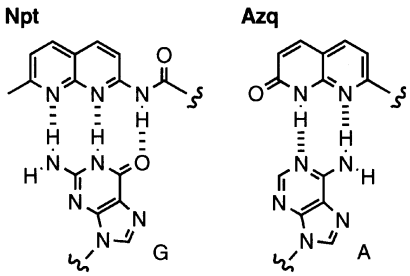

Figure 2. Hydrogen bonding patterns of **Npt**-G and **Azq**-A.

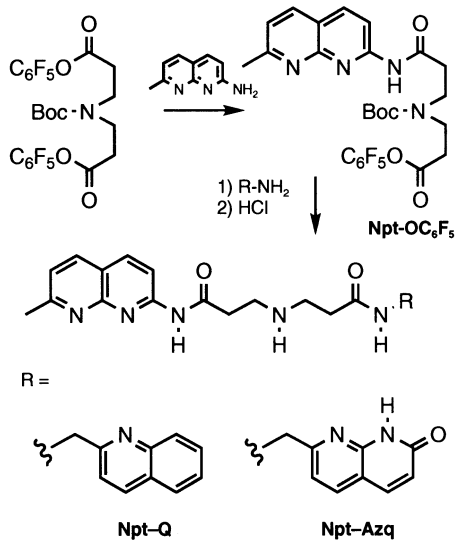

Figure 3. Synthetic scheme of **Npt**-based hybrids.

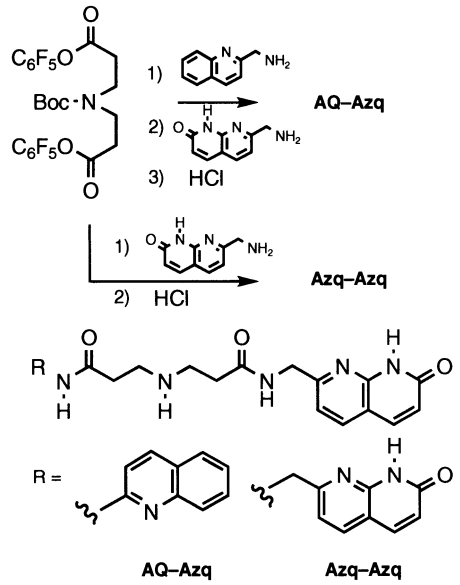

Figure 4. Synthetic scheme of **Azq**-based hybrids.

MATERIALS AND METHODS

Chemistry

In order to know the structure–activity relationship for the binding of **Npt–Azq** hybrid to G-A mismatches, hybrid molecules consisted of chromophores with different hydrogen-bonding groups were synthesized. These chromophores include **Npt**, **Azq**, quinoline (**Q**) and 2-aminoquinoline (**AQ**). Synthesis of the hybrid molecules consisting of **Npt** with **Azq** and other heterocycles is straightforward using *N*-(*tert*-butoxycarbonyl)imino-3,3′-bis(pentafluorophenyl propionate) (12), in which two carboxyl groups are activated as a pentafluorophenyl ester. Mono-substitution of the pentafluoroester with 2-amino-7-methylnaphthyridine produces intermediate amide **Npt**-OC_6F_5 that subsequently reacts with the heterocyclic amines to give hybrid ligands (Fig. 3). A similar procedure was used for the synthesis of **Azq**-based hybrid ligands (Fig. 4). Details of the synthetic procedure is described in the Supplementary Material.

Synthesis of Npt–Azq

To a solution of *N*-(*tert*-butoxycarbonyl)imino-3,3′-bis(pentafluorophenyl propionate) (1.5 g, 2.53 mmol) in dry DMF (5 ml) was added 2-amino-7-methyl-1,8-naphthyridine (180 mg, 1.14 mmol) and diisopropylethylamine (163 mg, 1.26 mmol). The reaction mixture was stirred at room temperature for 15 h. The solvent was evaporated to dryness and the residue was purified by column chromatography on silica gel to give **Npt**-OC_6F_5 (1.29 g, 90%) as pale yellow solids: ^{1}H-NMR ($CDCl_3$, 400 MHz) δ = 9.01 (br, 1H), 8.44 (d, 1H, *J* = 8.8 Hz), 8.12 (d, 1H, *J* = 8.8 Hz), 7.99 (d, 1H, *J* = 8.0 Hz), 7.26 (d, 1H, *J* = 8.0 Hz), 3.66 (m, 4H), 2.90 (m, 2H), 2.74 (m, 2H), 2.73 (s, 3H), 1.42 (s, 9H), ^{13}C-NMR ($CDCl_3$, 100 MHz) δ = 163.6, 155.3,

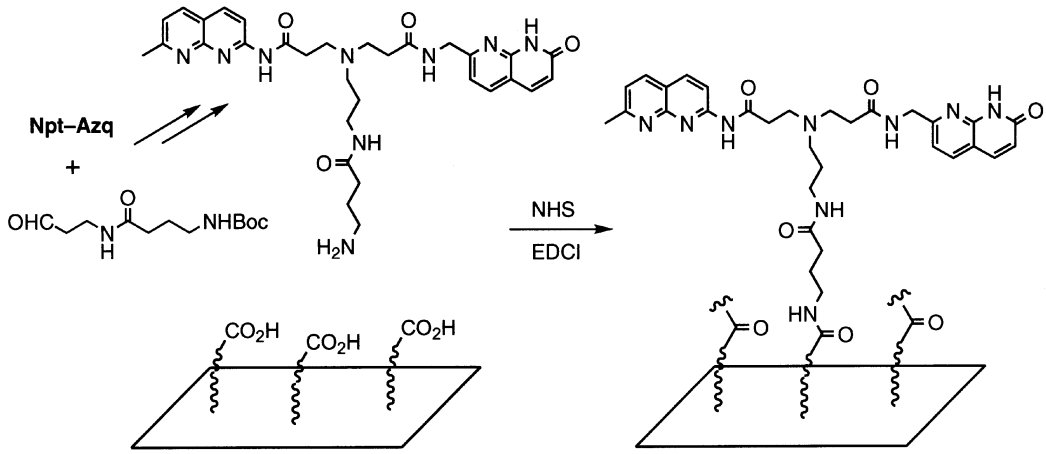

Figure 5. Synthetic scheme of **Npt–Azq** immobilized sensor surfaces.

154.6, 153.4, 142.6, 140.1, 139.5, 138.5, 136.6, 121.9, 118.8, 114.5, 80.9, 44.9, 44.4, 37.6, 37.2, 36.7, 33.4, 32.7, 28.6, 25.8, FABMS (NBA), *m/e* 569 [(M + H)$^+$], HRMS calc. for $C_{26}H_{26}O_5N_4F_5$ [(M + H)$^+$] 569.1821, found 569.1827.

To a solution of **Npt**-OC_6F_5 (300 mg, 0.53 mmol) in dry DMF (2 ml) was added 7-(aminomethyl)hydro-8-azaquinolin-2-one (93 mg, 0.53 mmol) and diisopropylethylamine (77 mg, 0.6 mmol). The reaction mixture was stirred at room temperature for 15 h. The solvent was evaporated to dryness and the residue was purified by column chromatography on silica gel to give ***N*-Boc-Npt–Azq** (227 mg, 77%) as pale yellow solids: ^{1}H-NMR ($CDCl_3$, 400 MHz) δ = 11.29 (br, 1H), 9.08 (br, 1H), 8.38 (d, 1H, *J* = 8.8 Hz), 8.06 (d, 1H, *J* = 8.0 Hz), 7.95 (d, 1H, *J* = 8.0 Hz), 7.81 (d, 1H, *J* = 8.0 Hz), 7.64 (d, 1H, *J* = 9.6 Hz), 7.27 (d, 1H, *J* = 8.0 Hz), 7.22 (d, 1H, *J* = 8.0 Hz), 6.64 (d, 1H, *J* = 9.6 Hz), 4.63 (d, 2H, *J* = 6.0 Hz), 3.58 (t, 2H, *J* = 6.8 Hz), 3.57 (t, 2H, *J* = 6.8 Hz), 2.71 (t, 2H, *J* = 6.8 Hz), 2.70 (s, 1H), 2.54 (t, 2H, *J* = 6.8 Hz), 1.36 (s, 9H), ^{13}C-NMR ($CDCl_3$, 100 MHz) δ = 171.7, 163.9, 163.4, 159.8, 155.7, 154.5, 153.6, 149.3, 139.3, 139.2, 137.4, 136.9, 123.1, 121.9, 118.8, 118.2, 114.6, 114.0, 80.5, 44.8, 41.8, 37.5, 28.6, 25.7, FABMS (NBA), *m/e* 560 [(M + H)$^+$], HRMS calc. for $C_{29}H_{34}O_5N_7$ [(M + H)$^+$] 560.2621, found 560.2618.

To a solution of ***N*-Boc-Npt–Azq** (62 mg, 0.11 mmol) in $CHCl_3$ (3 ml) was added ethyl acetate containing 4 M HCl (2 ml) at room temperature and the reaction mixture was stirred at room temperature for 0.5 h. The solvent was evaporated to dryness to give hydrochloride of **Npt–Azq** (quantitative yield) as white solids: ^{1}H-NMR ($CDCl_3$, 400 MHz) δ = 11.45 (br, 1H), 8.67 (t, 1H, *J* = 5.6 Hz), 8.31 (d, 1H, *J* = 8.8 Hz), 7.98 (d, 1H, *J* = 8.8 Hz), 7.88 (d, 1H, *J* = 8.0 Hz), 7.65 (d, 1H, *J* = 7.6 Hz), 7.53 (d, 1H, *J* = 9.6 Hz), 7.15 (d, 1H, *J* = 7.6 Hz), 7.14 (t, 1H, *J* = 8.0 Hz), 6.58 (d, 1H, *J* = 9.6 Hz), 4.65 (d, 2H, *J* = 5.6 Hz), 3.08 (t, 2H, *J* = 6.0 Hz), 3.06 (t, 2H, *J* = 6.0 Hz), 2.65 (t, 2H, *J* = 6.0 Hz), 2.58 (t, 2H, *J* = 6.0 Hz), 2.57 (s, 3H), ^{13}C NMR (CD_3OD, 100 MHz) δ = 171.8, 171,3, 165.0, 160.2, 159.7, 157.0, 148.5, 147.3, 146.4, 140.3, 140.2, 138.8, 122.5, 120.9, 120.2, 117.6, 117.0, 114.8, 44.1, 43.9, 43.1, 32.5, 30.5, 19.7, FABMS (NBA), *m/e* 460 [(M + H)$^+$], HRMS calc. for $C_{24}H_{26}O_3N_7$ [(M + H)$^+$] 460.2095, found 460.2097.

Synthesis of Npt–Azq having an aminoalkyl linker for immobilization onto SPR sensor surface

SPR sensors having **Npt–Azq** on their surface were synthesized to examine SPR detection of the G-A mismatch in a flow system (Fig. 5). **Npt–Azq** was immobilized on a dextran matrix coated gold surface (CM5 chip, BIAcore) through a bivalent linker of *N*-Boc-aminoaldehyde. First, **Npt–Azq** was tethered by a reductive amination to the linker, which was efficiently prepared from Boc-protected 4-aminobutanoic acid and 3-aminopropionaldehyde diethylacetal (Supplementary Material). Deprotection of a Boc group produced a primary amine, which was subsequently immobilized on the sensor surface by a coupling between the amino group and an activated carboxyl group on the CM5 chip using a standard method with 1-(3-dimethylaminopropyl)-3-ethylcarbodiimide hydrochloride (EDCI) and *N*-hydroxysuccinimide (NHS).

Preparation of a sensor chip carrying Npt–Azq on its surface

SPR measurements were performed with a BIAcore 2000 system (BIAcore, Uppsala, Sweden). Immobilization of **Npt–Azq** on a sensor chip CM5 (carboxymethylated dextran surface, BIAcore) was carried out using amine coupling kit (BIAcore) in a continuous flow of HBS-N buffer (10 mM HEPES, pH 7.4) containing NaCl (150 mM) at a flow rate of 10 µl/min. A solution (70 µl) of NHS (0.05 M) and EDCI (0.2 M) was injected using the QUICKINJECT command to activate the carboxymethylated dextran surface of a CM5 sensor chip. A solution (70 µl) of **Npt–Azq** having an aminoalkyl linker (2 mM in borate buffer, pH 9.2) was injected using the QUICKINJECT command on the activated surface. Residual activated surface was completely blocked by injection of a solution (20 µl) of ethanolamine hydrochloride (1.0 M, pH 8.5). Non-covalently bound material was removed by washing with 5 µl of 50 mM NaOH to produce the sensor chip carrying **Npt–Azq** on its surface. The amount of **Npt–Azq** immobilized on the surface was modulated by the reaction period of the immobilization, and was monitored as an increase of SPR signal [resonance unit (RU)] after the deactivation of the unreacted NHS-esters and a conditioning

Table 1. ΔT_m values for the duplexes containing **G-y** mismatches in the absence and presence of drugs[a]

Drug	**cGg/gAc**, T_m = 25.8°C	**cGg/gGc**, T_m = 25.1°C	**cGg/gCc**, T_m = 38.6°C
Npt–Azq	15.4 (0.6)	10.6 (0.7)	2.2 (0.8)
Npt–Npt	12.8 (1.0)	26.2 (1.0)	4.3 (1.0)
Npt–Q	1.6 (1.5)	4.5 (1.3)	2.0 (1.0)
AQ–Azq	–0.4 (0.4)	0.1 (0.1)	0.7 (0.4)
Azq–Azq	–0.5 (0.1)	–0.9 (0.7)	0.5 (0.6)
Npt	–0.6 (0.4)	–0.8 (0.2)	–0.3 (0.7)
Azq	0.3 (0.3)	0.3 (0.6)	0.4 (1.0)
Npt and **Azq**	–0.6 (0.5)	–0.8 (0.5)	–0.2 (0.1)

[a]T_m for the duplex 5′-d(CTAA **vGw** AATG)-3′/3′-d(GATT **xyz** TTAC)-5′ (5.0 μM each strand) in the absence (drug –) and presence (drug +) of drug (200 μM) was measured in 10 mM sodium cacodylate buffer (pH 7.0) containing 100 mM NaCl. $\Delta T_m = T_m$ (drug +) – T_m (drug –). The numbers in parentheses represent the maximum experimental error.

of the surface. Three sensor surfaces carrying **Npt–Azq** for 527, 722 and 951 RU were obtained by the immobilization for 1, 3 and 7 min with a 2 mM solution of **Npt–Azq** in a borate buffer (pH 9.2).

Measurements of thermal denaturation profiles of mismatch-containing duplexes

Thermal denaturation profiles of the duplexes 5′-d(CTAA **vGw** AATG)-3′/3′-d(GATT **xyz** TTAC)-5′ where G-**y** mismatches were flanked by **v-x** and **w-z** base pairs (4.5 or 5.0 μM for each strand) were measured in a sodium cacodylate buffer (10 mM, pH 7.0) containing NaCl (100 mM) using a Shimadzu UV-2550 UV-Vis spectrometer linked to a Peltier temperature controller. The absorbance of the sample was monitored at 260 nm from 4 to 70°C with a heating rate of 1°C/min in the absence and presence of a hybrid ligand. The measurements were carried out at the ligand concentration of 50 or 200 μM. The melting temperature of these duplexes was determined as the temperature crossing the melting curve and the median of two straight lines drawn for the single and duplex region in the melting curve.

General procedure for SPR binding experiments using synthetic oligonucleotides

All measurements were carried out at 25°C in a continuous flow of a buffer (10 mM HEPES, pH 7.4) containing NaCl (1 M) at a flow rate of 30 μl/min. A 1 μM solution of 27mer duplexes 5′-d(GTT ACA GAA TCT **VGW** AAG CCT AAT ACG)-3′/3′-d(CAA TGT CTT AGA **XYZ** TTC GGA TTA TGC)-5′ containing G-Y mismatches flanked by V-X and W-Z base pairs in the buffer were injected for 180 s for analyzing the association to the sensor surface. The buffer was subsequently injected for another 180 s for analyzing the dissociation of the bound oligomer form the surface. After each analysis, all binding materials were removed by washing with 30 μl of NaOH solution (50 mM). Immediately after washing, this system can be used for the next assay.

RESULTS AND DISCUSSION

UV melting temperature analyses

The bindings of **Npt–Azq** and other hybrid ligands to G-**y** mismatches were examined by measuring the melting temperature (T_m) of mismatch-containing duplexes (5.0 μM) in the presence of the ligand. The difference of the melting temperature (ΔT_m) in the absence and presence of the ligands is summarized in Table 1. A large ΔT_m of 26.2°C was obtained for the 11mer duplex containing the G-G mismatch flanked by two G-C base pairs (**vGw/xyz = cGg/gGc**) in the presence of **Npt–Npt**. In order to distinguish the 11mer duplexes used for the T_m measurements from the 27mer duplexes used for SPR studies, the flanking sequences to the mismatch of 11mer were described with lowercase letters, whereas uppercase letters were used of the flanking sequences of 27mer. Under these conditions, **Npt–Npt** also increased the T_m of the G-A mismatch (**cGg/gAc**) by 12.8°C, whereas only a modest ΔT_m of 4.3°C was observed for the matched duplex. In contrast to **Npt–Npt**, substitution of one **Npt** chromophore to **Azq** in **Npt–Azq** showed a striking difference in the spectrum for mismatch stabilization. **Npt–Azq** strongly stabilizes **cGg/gAc** as indicated by the ΔT_m of 15.4°C, exceeding the ΔT_m of **Npt–Npt** by 2.6°C. Since the non-specific binding to a fully matched duplex is weaker for **Npt–Azq** (2.2°C) than **Npt–Npt** (4.3°C), **Npt–Azq** is currently the strongest ligand described that stabilizes the G-A mismatch.

To gain insight into a role of **Azq** chromophore for the binding to the G-A mismatch, the **Azq** and **Npt** chromophores in **Npt–Azq** were replaced by either quinoline (**Q**) or aminoquinoline (**AQ**) chromophores. A dramatic decrease of the ΔT_m from 15.4 to 1.6°C was observed by replacing **Azq** chromophore in **Npt–Azq** with **Q** in **Npt–Q**. The hydrogen-bonding donor of N-H in **Azq** was replaced by a non-hydrogen bonding group of C-H. Aminoquinoline–azaquinolone (**AQ–Azq**) obtained by a substitution of **Npt** in **Npt–Azq** with **AQ** completely lost the binding to both G-A and G-G mismatches (Fig. 6). Furthermore, the azaquinolone dimer (**Azq–Azq**), the single chromophore **Npt** and **Azq**, or the 1:1 mixture of **Npt** and **Azq** did not stabilize the G-A mismatch. These results clearly indicated that a covalent attachment of **Npt** and **Azq** chromophores is essential for the stabilization of the G-A mismatch. These remarkable effects of the substitution of the **Npt** and **Azq** chromophores in **Npt–Azq** on the stabilization of the G-A mismatch suggests the significance of the hydrogen bonding of **Azq** to adenine and **Npt** to guanine (Fig. 2). It has been recently shown that **Azq** is superior to thymine in the recognition of adenine in duplex and triplex structure (21). These observations are well consistent to our results.

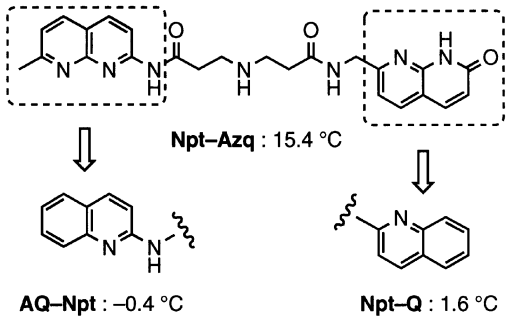

Figure 6. Schematic representation of the effect of structural modification of chromophores in **Npt–Azq** on the increased melting temperature (ΔT_m) of the G-A mismatch.

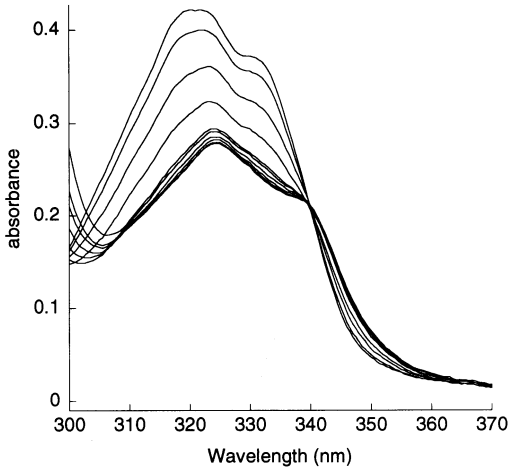

Figure 7. UV absorption spectra of **Npt–Azq** (20 μM) in the presence of different concentrations of the G-A mismatch duplex **cGg/gAc** (0–50 μM). The experiments were conducted in a sodium cacodylate buffer (10 mM, pH 7.0) containing NaCl (100 mM) at 15°C. The concentrations of DNA are 0, 1, 2.5, 5, 7.5, 10, 15, 20, 25 and 37.5 μM.

Evaluation of the binding of Npt–Azq to G-A mismatches

Having found that **Npt–Azq** strongly stabilizes the G-A mismatch, and that the hydrogen bonding groups in the two chromophores are essential, the binding of the ligand was studied in detail. First, the UV absorption of the **Npt–Azq** (20 μM) was measured in the presence of different concentrations of the 11mer G-A mismatch duplex (**cGg/gAc**) (0–50 μM). In the absence of DNA, the ligand showed an absorption maximum at 320 nm and a shoulder at 333 nm. At increasing **cGg/gAc** concentrations, these absorptions decreased in intensity with a concomitant red shift of the peak from 320 to 324 nm (Fig. 7). An isosbestic point was observed at 340 nm for the spectral change, indicating that UV absorbance of **Npt–Azq** linearly changes from the free state to the bound state to **cGg/gAc**. With the data points at 320 nm, the fraction of the total ligand bound against the molar fraction of **cGg/gAc** ([**cGg/gAc**] / [**Npt–Azq**]) was plotted (Fig. 8). The bound fraction of **Npt–Azq** rapidly increased with increasing **cGg/gAc** concentration and saturated in the presence of approximately one molar equivalent of DNA. In contrast, the bound fraction of **Npt–Npt** to the G-A mismatch

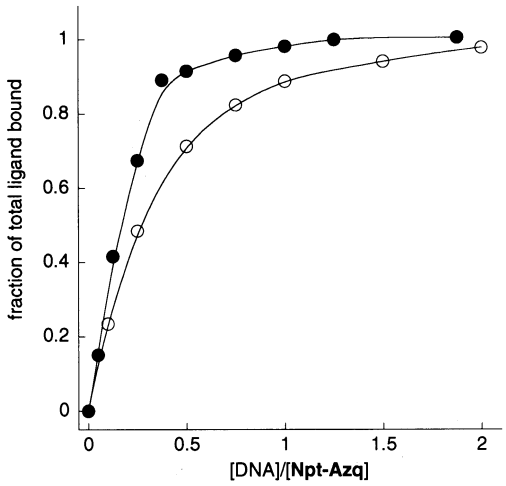

Figure 8. Plot of the fraction of total ligand bound against the molar fraction of the G-A mismatch duplex **cGg/gAc** to the concentration of **Npt–Azq** (filled circles) and **Npt–Npt** (open circles), respectively. The data were obtained from experiments shown in Figure 7.

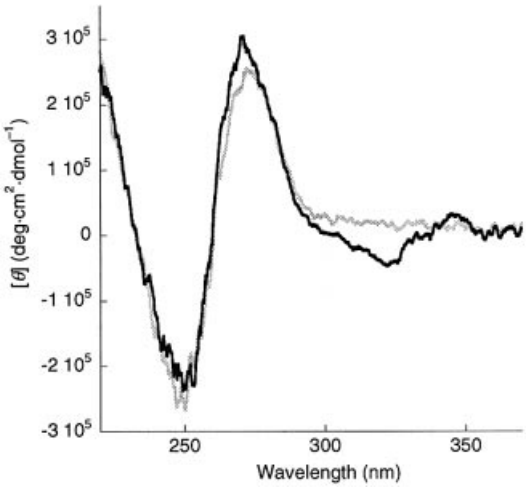

Figure 9. CD spectra of **cGg/gAc** (4.5 μM) measured in 10 mM sodium cacodylate buffer (pH 7.0) and 100 mM NaCl at 25°C in the absence (gray) and presence (black) of 20 μM **Npt–Azq**.

steadily increased with increasing **cGg/gAc** concentration and reached saturation with two molar equivalents of DNA. This suggests that the binding of **Npt–Azq** to the G-A mismatch is stronger than that of **Npt–Npt**. CD spectra of **cGg/gAc** in the presence of **Npt–Azq** showed an increase of the ellipticity at 275 nm in addition to strong and weak CD signals induced at 320 and 345 nm, respectively (Fig. 9). Distinct induced CD signals indicated that **Npt–Azq** was under the influence of the chiral environment of duplex DNA in the complex.

The effect of the concentration of **Npt–Azq** on the ΔT_m of **cGg/gAc** was examined by measuring the melting curve at different drug concentrations. Increasing the concentration of **Npt–Azq**, the ΔT_m of the duplex increased and reached a plateau (Fig. 10). At 50 μM **Npt–Azq**, UV-melting profiles were obtained for all G-A mismatches with regard to the sequence flanking to the mismatch (**vGw/xAz**). The T_m of all G-A mismatches except for **tGt/aAa** in the absence and

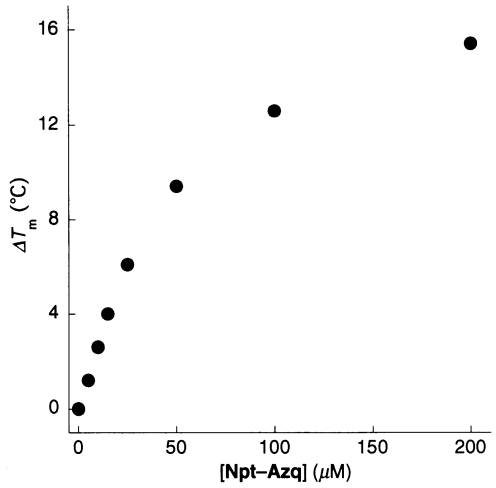

Figure 10. Concentration dependency of ΔT_m of **cGg/gAc** (4.5 μM). The melting temperature of **cGg/gAc** (4.5 μM) was measured in the presence of 0, 5, 10, 15, 25, 50, 100 and 200 μM **Npt–Azq** in 10 mM sodium cacodylate (pH 7.0) and 100 mM NaCl.

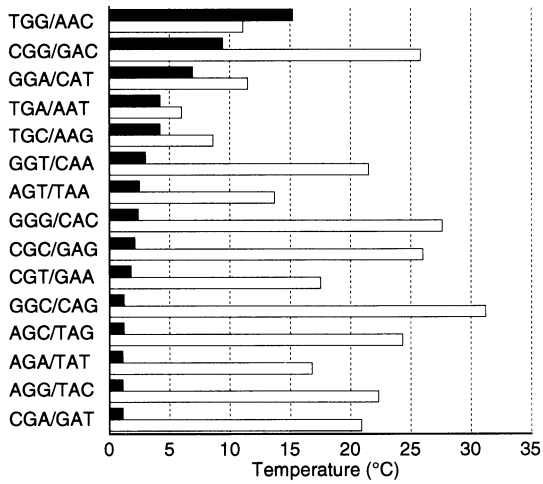

Figure 11. ΔT_m values for G-A mismatches (4.5 μM) of different flanking sequence in the presence of **Npt–Azq** (50 μM) (black) and melting temperatures of G-A mismatches in the absence of **Npt–Azq** (white).

presence of **Npt–Azq** are summarized in Figure 11. The T_m of **tGt/aAa** was too low to measure under the conditions. The largest ΔT_m was recorded for the sequence of **tGg/aAc**. The sequence **cGg/gAc** we have examined in detail had the second largest ΔT_m value. While we have anticipated that the binding of **Npt–Azq** would be favorable for the G-A mismatches flanking to G-C base pairs due to the increased stacking stabilization of the complex, there seems no obvious rationalization for the sequences stabilized by the drug. The melting curves of the sequences showing the top five ΔT_m values are shown in Figure 12. The energy gains of these five G-A mismatches in the presence of 50 μM **Npt–Azq** were estimated by curve fitting of the melting profiles. The melting profile of the G-A mismatch in the absence and presence of **Npt–Azq** were fitted to a two-state model with a non-linear least-squares program by using Sigma Plots (version 2001) (22). The energy gains obtained by these simulations are

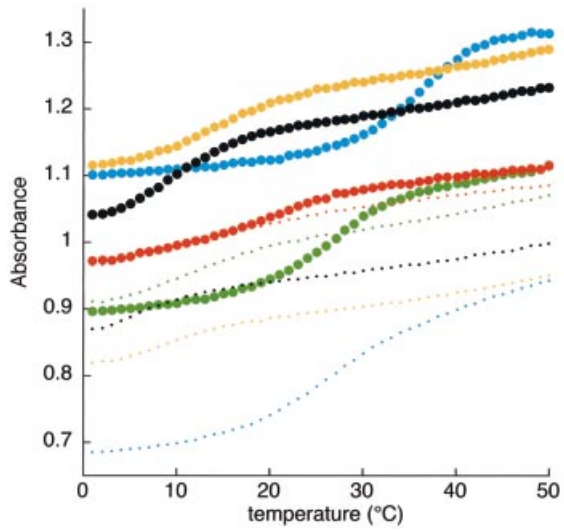

Figure 12. Melting curves of G-A mismatch duplexes (4.5 μM) in the absence (dots) and presence (filled circles) of **Npt–Azq** (50 μM) in 10 mM sodium cacodylate (pH 7.0) and 100 mM NaCl. **tGg/aAc**, green; **cGg/gAc**, blue; **gGa/cAt**, red; **tGc/aAg**, orange; **tGa/aAt**, black.

Table 2. Estimated energy gains of the G-A mismatches in the presence of 50 μM **Npt–Azq**[a]

G-A mismatch	ΔG (drug –)	ΔG (drug +)	$\Delta\Delta G$
cGg/gAc	–9.7	–15.7	–6.0
tGc/aAg	–10.5	–14.6	–4.1
tGg/aAc	–8.4	–12.1	–3.6
gGa/cAt	–6.0	–8.9	–2.9
tGa/aAt	–8.1	–9.8	–1.7

[a]ΔG (drug –) and ΔG (drug +) were obtained by curve fitting of the melting profiles in the absence and presence of **Npt–Azq** (50 μM) at 277.15 K and reported in kcal/mol. $\Delta\Delta G = \Delta G$ (drug +) – ΔG (drug –).

summarized in Table 2. The largest energy gain of –6.0 kcal/mol (277.15 K) was obtained for **cGg/gAc**, whereas the sequence **tGg/aAc**, which recorded the highest ΔT_m value, was ranked third. As we reported earlier, the magnitude of ΔT_m is not consistent with the energy gain by the drug binding especially when the duplex showed a low melting temperature (23).

SPR analyses

Having discovered that **Npt–Azq** strongly stabilizes the G-A mismatch DNA, the binding of G-containing mismatches to the SPR sensor where **Npt–Azq** was immobilized on the surfaces was investigated. SPR analyses of a 1 μM solution of 27mer duplexes 5′-d(GTT ACA GAA TCT **VGW** AAG CCT AAT ACG)-3′/3′-d(CAA TGT CTT AGA **XYZ** TTC GGA TTA TGC)-5′ containing a G-Y mismatch flanked by G-C base pairs (5′-**VGW**-3′/3′-**XYZ**-5′ = CGG/GYC, Y = A, G or C) were performed with the sensor carrying **Npt–Azq** for 951 RU on the surface. To suppress a non-specific absorption of DNA to the sensor surface, binding experiments were carried out under high salt conditions (1 M NaCl and 10 mM HEPES buffer, pH 7.4). A sensorgram obtained for the G-A mismatch (**CGG/GAC**) showed strong SPR signals, of which intensity reached to 193 RU, after 180 s of the association time

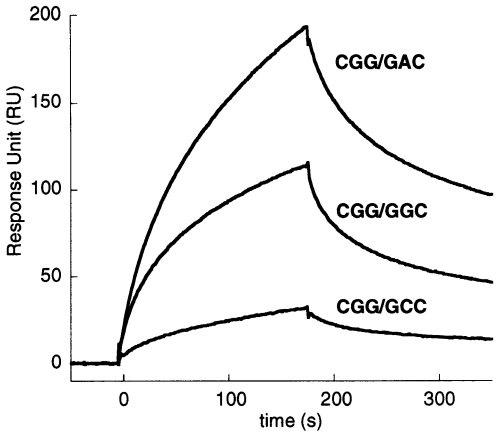

Figure 13. Sensorgrams for the binding of duplexes containing G-Y mismatches to the **Npt–Azq** immobilized SPR sensor surface. Aliquots of 90 µl of the duplexes (1.0 µM in 10 mM HEPES buffer pH 7.4, 1 M NaCl) containing G-A, G-G mismatch and G-C matches were injected for 180 s to measure the association to the sensor surface.

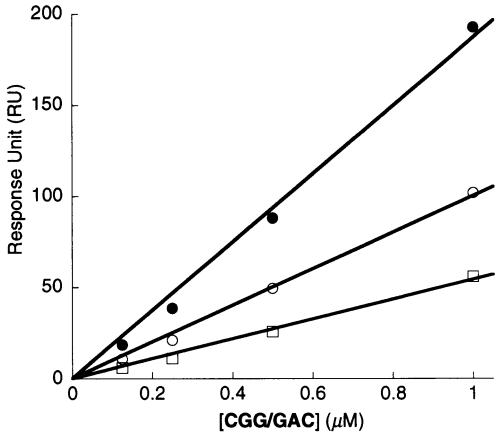

Figure 14. Concentration dependency for the SPR responses for 27mer duplex (**CGG/GAC**) containing a G-A mismatch. **CGG/GAC** at concentrations of 0.13, 0.25, 0.5 and 1.0 µM were analyzed by three sensors carrying **Npt–Azq** for 951 (filled circles), 722 (open circles) and 527 RU (squares) on the surface. Responses after 180 s of the association time were plotted against the DNA concentration.

(Fig. 13). The SPR signal for the G-G mismatch (**CGG/GGC**) was also distinct, but much lower in intensity (114 RU) than that obtained for **CGG/GAC**. In marked contrast, only a weak SPR signal (31 RU) was observed for the G-C match DNA (**CGG/GCC**). These results are consistent with those of UV-melting studies in the presence of **Npt–Azq** showing a higher ΔT_m for **cGg/gAc** than for **cGg/gGc** and almost negligible stabilization for the G-C match DNA. The distinct differences in the intensity of the SPR signal between the G-A mismatch and G-C match DNA clearly indicate a unique character of the **Npt–Azq** immobilized sensor surface.

Concentration dependency for the SPR responses

To further evaluate the fidelity of the novel sensor surfaces detecting the G-A mismatches, the concentration dependency of the SPR signal for the binding of the G-A mismatch to the sensor surface was investigated. The duplex **CGG/GAC** containing a G-A mismatch of different concentrations (0.13–1.0 µM) was analyzed by three sensor surfaces carrying **Npt–Azq** for 951, 722 and 527 RU. The SPR responses after the association time of 180 s were plotted against the concentration of the G-A mismatch DNA (Fig. 14). The SPR signals produced by each sensor surface clearly showed a linear correlation to the concentration of **CGG/GAC**, with a correlation coefficient of 0.99. A linear correlation between SPR intensity and DNA concentrations validated that the observed SPR signals were definitely due to a specific interaction between **CGG/GAC** and **Npt–Azq** on the sensor surface. Furthermore, it was suggested that the sensor surface is not only effective to detect the G-A mismatch, but also applicable to quantify G-A mismatch DNA at the concentration range up to 1 µM (24). It is worth noting that the SPR responses of three sensor surfaces were not proportional to the amount of **Npt–Azq** immobilized on the surface. This is most likely due to the different surfaces of the three sensors produced by independent immobilization processes for the three CM5 chips of research grade. Thus, calibration of the sensor surface is necessary for quantitative applications.

Effect of the flanking sequence to the G-A mismatch on the SPR responses

To know the scope and limitation of the novel G-A mismatch detecting sensor, the effect of the sequence flanking to the mismatch on the binding to the **Npt–Azq** immobilized sensor surface was examined. In heteroduplex analyses, it is important to differentiate the mismatch-containing duplex from the fully matched duplex. Thus, the SPR signal of a mismatched duplex relative to that of the fully matched duplex was investigated. DNA duplexes containing G-A mismatches in the sequence of 5′-**VGW**-3′/3′-**XAZ**-5′ were analyzed by SPR using an **Npt–Azq** immobilized sensor surface. SPR intensities of 16 G-A mismatches were reported by the relative intensity to the highest signal of the fully matched duplex. G-A mismatches are largely divided into three groups with regard to the affinity to the surface. The first group of G-A mismatches showed a strong response to the **Npt–Azq** immobilized surfaces. Among 16 duplexes, the strongest SPR signal was observed for **TGG/AAC** (Fig. 15a). The SPR intensity was more than two times stronger than the signal for **CGG/GAC**, and 12-fold stronger than that observed for the matched duplex. Besides these two, G-A mismatches in **GGA/CAT**, **TGC/AAG**, **AGG/TAC** and **AGA/TAT** showed SPR signals that are markedly stronger than the signal of a matched duplex by >2-fold. The fitting of the response curve to a 1:1 Langmuir model with BIAevaluation software (version 3) provided an estimate of the association constant (K_a) of each G-A mismatch to the **Npt–Azq** immobilized surface. The K_a obtained for the G-A mismatches were 1.8×10^6 M^{-1} for **TGG/AAC**, 1.0×10^6 M^{-1} for **CGG/GAC**, 9.0×10^5 M^{-1} for **GGA/CAT**, 9.2×10^5 M^{-1} for **AGG/TAC** 7.5×10^5 M^{-1} for **AGA/TAT**. The K_a for the **TGC/AAG** could not be estimated due to a very slow dissociation of DNA from the surface. The second group of G-A mismatches showed reduced relative intensities compared with those in the first group (Fig. 15b). The SPR responses of **AGT/TAA** and **GGG/CAC** are clearly distinguished from that of matched duplex. The relative intensity of the SPR signal to the mismatches is ~1.5-fold. The

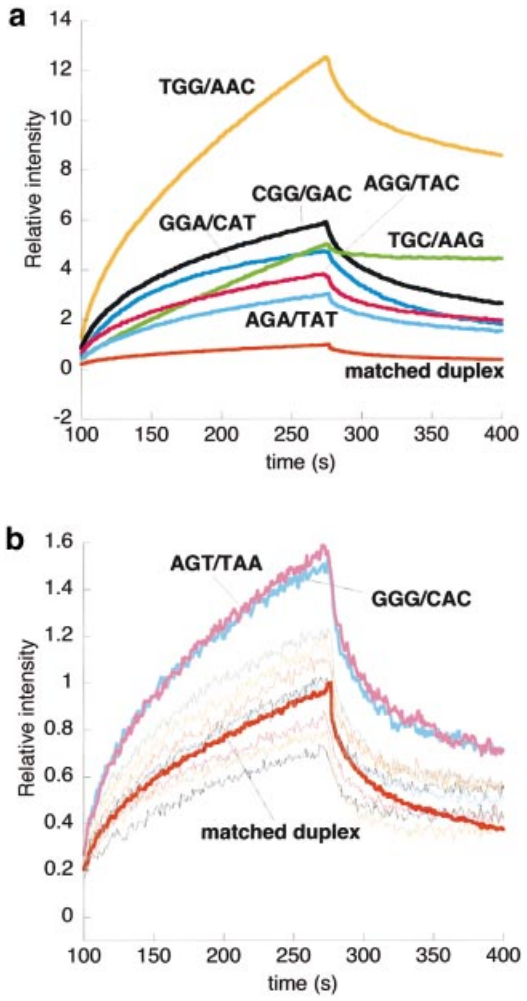

Figure 15. Relative SPR intensities of the binding of G-A mismatches to the **Npt–Azq** immobilized sensor surfaces. G-A mismatches (1 μM) were analyzed in HEPES buffer for 180 s of association to the sensor surface and then dissociation of the bound DNA from the surfaces. SPR intensities were reported as a relative intensity by setting the maximum intensity of the fully matched duplex to be 1.0. (**a**) G-A mismatches strongly bind to the sensor. **TGG/AAC**, yellow; **CGG/GAC**, black; **TGC/AAG**, green; **GGA/CAT**, blue; **AGG/TAC**, pink; **AGA/TAT**, aqua; matched duplex, red. (**b**) G-A mismatches with weak binding to the sensor. **AGT/TAA**, violet; **GGG/CAC**, aqua; matched duplex, red.

third group of mismatches did not show any noticeable differences in SPR intensity from that of fully matched duplex. These analyses showed that the sensor we reported here would be effective to detect G-A mismatches in eight flanking sequences, covering 50% of all G-A mismatches.

A sequence-dependent binding of **Npt–Azq** to the G-A mismatches implies that **Npt–Azq** not only binds to the G-A mismatches, but also interacts to the bases flanking to the mismatch. SPR analyses showed that the binding kinetics for the G-A mismatch in **TGC/AAG** are markedly different from those of other G-A mismatches. The association of **TGC/AAG** to the **Npt–Azq** immobilized surface and the dissociation from the surface was quite slow. These observations are particularly important for the molecular design of the improved version of **Npt–Azq** that is aiming to detect the rest of the eight G-A mismatches.

Conclusion

The new molecule **Npt–Azq** was discovered to be the ligand strongly stabilizing the G-A mismatch. The SPR sensor surface on which **Npt–Azq** was immobilized was the first sensor detecting the G-A mismatch in duplex DNA. The G-A mismatch is produced by a heteroduplex formation from a pair of duplex DNAs containing a G·C to T·A mutation. The G to T transversion is high in frequency because the oxidation of guanine leading to a formation of 8-oxoguanine eventually resulted in the mutation (25). Oxidation of guanine is known to be sensitively affected by the base 3′ side to the guanine (26). The 5′-GG-3′ is most easily oxidizable and the 5′-GA-3′ is second in 5′-GX-3′ sequences. The G in the G-A mismatches that are detectable by the SPR surface are mostly flanked by 3′ side G and A, suggesting that the oxidation at those Gs is high in frequency. Thus, the **Npt–Azq** immobilized sensor surface reported here would be a useful and important tool for the discovery of a G to T mutation by detecting the G-A mismatches.

SUPPLEMENTARY MATERIAL

Supplementary Material is available at NAR Online.

ACKNOWLEDGEMENTS

This work was supported by Grant-in-Aid for Scientific Research on Priority Areas (C) ‘Medical Genome Science’ from the Ministry of Education, Culture, Sports, Science and Technology of Japan.

REFERENCES

1. Syvänen,A.-C. (2001) Accessing genetic variation: genotyping single nucleotide polymorphisms. *Nature Rev. Genet.*, **2**, 930–942.
2. Kwok,P.Y. (2001) Methods for genotyping single nucleotide polymorphisms. *Annu. Rev. Genom. Hum. Genet.*, **2**, 235–258.
3. Schafer,A.J. and Hawkins,J.R. (1998) DNA variation and the future of human genetics. *Nat. Biotechnol.*, **16**, 33–39.
4. Nakatani,K., Sando,S. and Saito,I. (2001) Scanning of guanine-guanine mismatches in DNA by synthetic ligands using surface plasmon resonance assay. *Nat. Biotechnol.*, **19**, 51–55.
5. Nataraj,A.J., Olivos-Glander,I., Kusukawa,N. and Highsmith,W.E.,Jr (1999) Single-strand conformation polymorphism and heteroduplex analysis for gel-based mutation detection. *Electrophoresis*, **20**, 1177–1185.
6. White,M.B., Carvalho,M., Derse,D., O’Brien,S.J. and Dean,M. (1992) Detecting single base substitution as heteroduplex polymorphisms. *Genomics*, **12**, 301–306.
7. Myers,R.M., Larin,Z. and Maniatis,T., (1985) Detection of single base substitutions by ribonuclease cleavage at mismatches in RNA–DNA duplexes. *Science*, **230**, 1242–1246.
8. Rowley,G., Saad,S., Giannelli,F. and Green,P.M., (1995) Ultrarapid mutation detection by multiplex, solid-phase chemical cleavage. *Genomics*, **30**, 574–582.
9. Roberts,E., Deeble,V.J., Woods,C.G. and Taylor,G.R. (1997) Potassium permanganate and tetraethylammonium chloride are a safe and effective substitute for osmium tetroxide in solid-phase fluorescent chemical cleavage of mismatch. *Nucleic Acids Res.*, **25**, 3377–3378.
10. Fazakerley,G.V., Qignard,E., Woisard,A., Guschlbauer,W., van der Marel,G.A., van Boom,J.H., Jones,M. and Radman,M. (1986) Structures of mismatched base pairs in DNA and their recognition by the *Escherichia coli* mismatch repair system. *EMBO J.*, **5**, 3697–3703.
11. Smith,J. and Modrich,P. (1996) Mutation detection with MutH, MutL and MutS mismatch repair proteins. *Proc. Natl Acad. Sci. USA*, **93**, 4374–4379.

12. Nakatani,K., Sando,S., Kumasawa,H., Kikuchi,J. and Saito,I. (2001) Recognition of guanine-guanine mismatches by dimeric form of 2-amino-1,8-naphthyridine. *J. Am. Chem. Soc.*, **123**, 12650–12657.
13. Nakatani,K., Sando,S. and Saito,I. (2000) Recognition of a single guanine bulge by 2-acylamino-1,8-naphthyridine. *J. Am. Chem. Soc.*, **122**, 2172–2177.
14. Nakatani,K., Hagihara,S., Sando,S., Sakamoto,S., Yamaguchi,K., Maesawa,C. and Saito,I. (2003) Induction of a remarkable conformational change in a human telomeric sequence by the binding of naphthyridine dimer: inhibition of the elongation of a telomeric repeat by telomerase. *J. Am. Chem. Soc.*, **125**, 662–666.
15. Smith,E.A., Kyo,M., Kumasawa,H., Nakatani,K., Saito,I. and Corn,R.M. (2002) Chemically induced hairpin formation in DNA monolayers. *J. Am. Chem. Soc.*, **124**, 6810–6811.
16. Nakatani,K., Horie,S. and Saito,I. (2003) Affinity labeling of single guanine bulge. *J. Am. Chem. Soc.*, **125**, 8972–8973.
17. Jackson,B.A. and Barton,J.K. (2000) Recognition of base mismatches in DNA by 5,6-chrysenequinone diimine complexes of rhodium(III): a proposed mechanism for preferential binding in destabilized regions of the double helix. *Biochemistry*, **39**, 6176–6182.
18. Jackson,B.A. and Barton,J.K. (1997) Recognition of DNA base mismatches by a rhodium intercalator. *J. Am. Chem. Soc.*, **119**, 12986–12987.
19. Jackson,B.A., Alekseyev,V.Y. and Barton,J.K. (1999) A versatile mismatch recognition agent: specific cleavage of a plasmid DNA at a single base mispair. *Biochemistry*, **38**, 4655–4662.
20. Lacy,E.R., Cox,K.K., Wilson,W.D. and Lee.M. (2002) Recognition of T·G mismatched base pairs in DNA by stacked imidazole-containing polyamides: surface plasmon resonance and circular dichroism studies. *Nucleic Acids Res.*, **30**, 1834–1841.
21. Eldrup,A.B., Christensen,C., Haaima,G. and Nielsen,P.E. (2002) Substituted 1,8-naphthyridin-2(1*H*)-ones are superior to thymine in the recognition of adenine in duplex as well as triplex structures. *J. Am. Chem. Soc.*, **124**, 3254–3262.
22. Marky,L.A. and Breslauer,K.J. (1987) Calculating thermodynamic data for transitions of any molecularity from equilibrium melting curves. *Biopolymers*, **26**, 1601–1620.
23. Nakatani,K., Horie,S., Murase,T., Hagihara,S. and Saito,I. (2003) Assessment of the sequence dependency for the binding of 2-aminonaphthyridine to the guanine bulge. *Bioorg. Med. Chem.*, **11**, 2347–2353.
24. Zhu,G., Yang,B. and Jennings,R.N. (2000) Quantitation of basic fibroblast growth factor by immunoassay using BIAcore 2000. *J. Pharm. Biomed. Anal.*, **24**, 281–290.
25. Friedberg,E.C., Walker,G.C. and Siede,W. (1995) *DNA Repair and Mutagenesis*. ASM Press, Washington, DC, pp. 1–58.
26. Saito,I., Takayama,M., Sugiyama,H., Nakatani,K., Tsuchida,A. and Yamamoto,M. (1995) Photoinduced DNA cleavage via electron transfer: demonstration that guanine residues located 5′ to guanine are the most electron-donating sites. *J. Am. Chem. Soc.*, **117**, 6406–6407.